

**Spin trapping of radical intermediates in gas phase catalysis:  
cyclohexane oxidation over metal oxides**

**Marco Conte and Victor Chechik\***

\* *Department of Chemistry, University of York, Heslington, York, YO10 5DD, United Kingdom, Tel: +44 1904 434185; E-mail: [vc4@york.ac.uk](mailto:vc4@york.ac.uk)*

**Table of contents**

Materials and methods: chemicals; spin trapping reactor, spin trapping and EPR experiments; MoO<sub>3</sub> activity test and products characterization *via* GC; EPR spectra deconvolution; control tests.

**Figures and tables:**

**Figure S1:** GC analysis of the reactor effluents for the oxidation of cyclohexane over MoO<sub>3</sub> at 180 °C in air.

**Figure S2:** EPR spectrum deconvolution of the spin adducts obtained during cyclohexane oxidation over MoO<sub>3</sub> at 180 °C in aerobic conditions.

**Figure S3:** EPR spin trapping control test experiments, using feeding the reactor with cyclohexanol, cyclohexanone and reactor with no catalyst.

**Figure S4:** estimation of radical lifetime

**Figure S5:** EPR spectrum deconvolution of the spin adducts obtained during cyclohexane oxidation over MoO<sub>3</sub> at 180 °C in anaerobic conditions.

**Figure S6:** spin adducts spectra for the cyclohexane oxidation in air at 180 °C over MoO<sub>3</sub>, Cr<sub>2</sub>O<sub>3</sub> and WO<sub>3</sub>, using DMPO as spin trap.

**Figure S7:** spin adducts spectra for the cyclohexane oxidation in air at 180 °C over MoO<sub>3</sub>, Cr<sub>2</sub>O<sub>3</sub> and WO<sub>3</sub>, using PBN as spin trap.

**Figure S8:** spin adducts spectra for the *n*-hexane oxidation in air at 180 °C over MoO<sub>3</sub>, Cr<sub>2</sub>O<sub>3</sub> and WO<sub>3</sub>, using DMPO as spin trap.

**Figure S9:** EPR spectrum deconvolution of the spin adducts obtained during cyclohexane oxidation over MoO<sub>3</sub> pre-treated with nitrogen.

## Chemicals

DMPO, PBN, MoO<sub>3</sub>, Cr<sub>2</sub>O<sub>3</sub>, WO<sub>3</sub> and other chemicals were purchased from Aldrich and used without further purification.

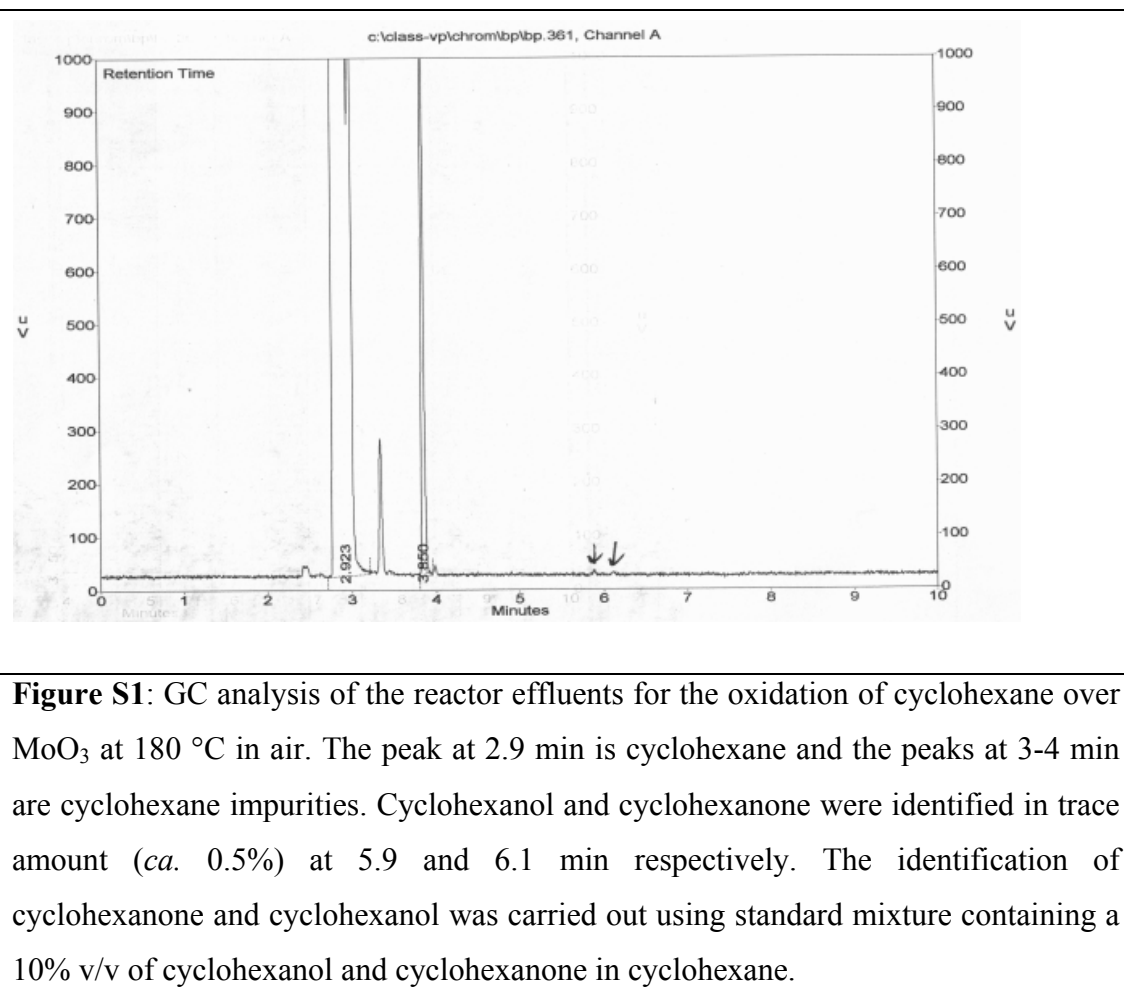
## Spin trapping reactor

The spin trapping reactor was made of a stainless steel tube with internal diameter of 4.83 mm with the catalytic bed of the metal oxide (20 mg) placed above a silica wool layer at the bottom. The silica wool layer was placed on a metal grid in order to avoid any transfer or the metal oxide to the spin trapping solution. The thickness of the metal oxide layer was *ca.* 1 mm. The reactor was fed from the top *via* a saturator containing the substrate under N<sub>2</sub> flow. The reactor was heated up to 180 °C *via* heating tape. The bottom of the catalytic bed was monolithically joined to a tube of an internal diameter of 2.23 mm in order to increase the linear velocity of the effluents, and cooled using a brass heat exchanger fed with cold water. This allowed cooling the reactor effluents from 180 °C to 22 °C. The reactor outlet was then joined to a PTFE tube (the standard tests were carried out on a Swagelock OD 1/8", ID 2.23 mm which has the same dimensional values of the stainless steel) immersed in a toluene/DMPO solution. The solution was then concentrated and analysed *via* X-band EPR spectroscopy.

Using these reactor dimensions, it is possible to calculate the time of flight of the radical species (50 to 25 ms moving from 500 to 1000 mL/min inlet flow) and the time of contact of the substrate with the catalytic bed (2.2 to 1.2 ms moving from 500 to 1000 mL/min). It should be noted that an inlet flow of 1000 mL/min lead to a gas hourly space velocity (GHSV) of *ca.*  $3.3 \times 10^9$  h<sup>-1</sup>, which is  $10^4$  -  $10^6$  times higher than the typical values used in gas phase microreactors to evaluate conversion and selectivity of an heterogeneous catalyst. However, this high value is needed to ensure fast transport of the radicals into trapping solution which is essential for detection. The lifetime of the radicals in gas phase was evaluated as *ca.* 20-80 ms depending on the species trapped (see figure S3).

### GC analysis of the reactor effluents

To emulate the spin trapping reaction conditions, MoO<sub>3</sub> (20 mg) was used at 180 °C with an air inlet flow of 1000 mL/min. The saturator was fed with 4 mL of cyclohexane heated to 40 °C. The reactor effluents were condensed and collected in a cold trap at 0 °C. The reaction mixture was analysed by gas chromatography using a Shimadzu instrument with an initial column temperature of 50 °C and a final column temperature of 350 °C. The temperature ramp was 5 °C/min and the final temperature was held for 20 min. Injector and detector temperatures were both 350 °C. The column used to carry out the separation was a Zebron ZB-5 w/guardian, (30m length, 0.25 mm internal diameter and 0.25 µm film thickness).



### EPR and spin trapping experiments

X-band EPR spectra were recorded at room temperature in deoxygenated toluene, using a Bruker ESP-300E spectrometer. The typical instrument parameters were as follows: centre field 3485 G, sweep width 100 G, sweep time 82 s, time constant 20 ms, power 5 mW, modulation frequency 100 kHz, modulation width 0.97 G. Quantitative spectral analysis was carried out using WinSim software.<sup>1</sup>

The spin trapping experiments were performed as follows: the reactor effluents were collected in a DMPO/toluene solution (50 µL of DMPO in 2 mL of toluene). The collection was carried out up to total consumption of the substrate in the saturator (23 min were required when cyclohexane was used, saturator heated at 40 °C at inlet flow of air or N<sub>2</sub> of 1000 mL/min). The resulting solution was then concentrated using a rotary evaporator to a final volume of 200 µL, transferred into a glass tube and deoxygenated by bubbling nitrogen for *ca.* 1 min before recording the EPR spectra.

### Spin trapping under aerobic conditions

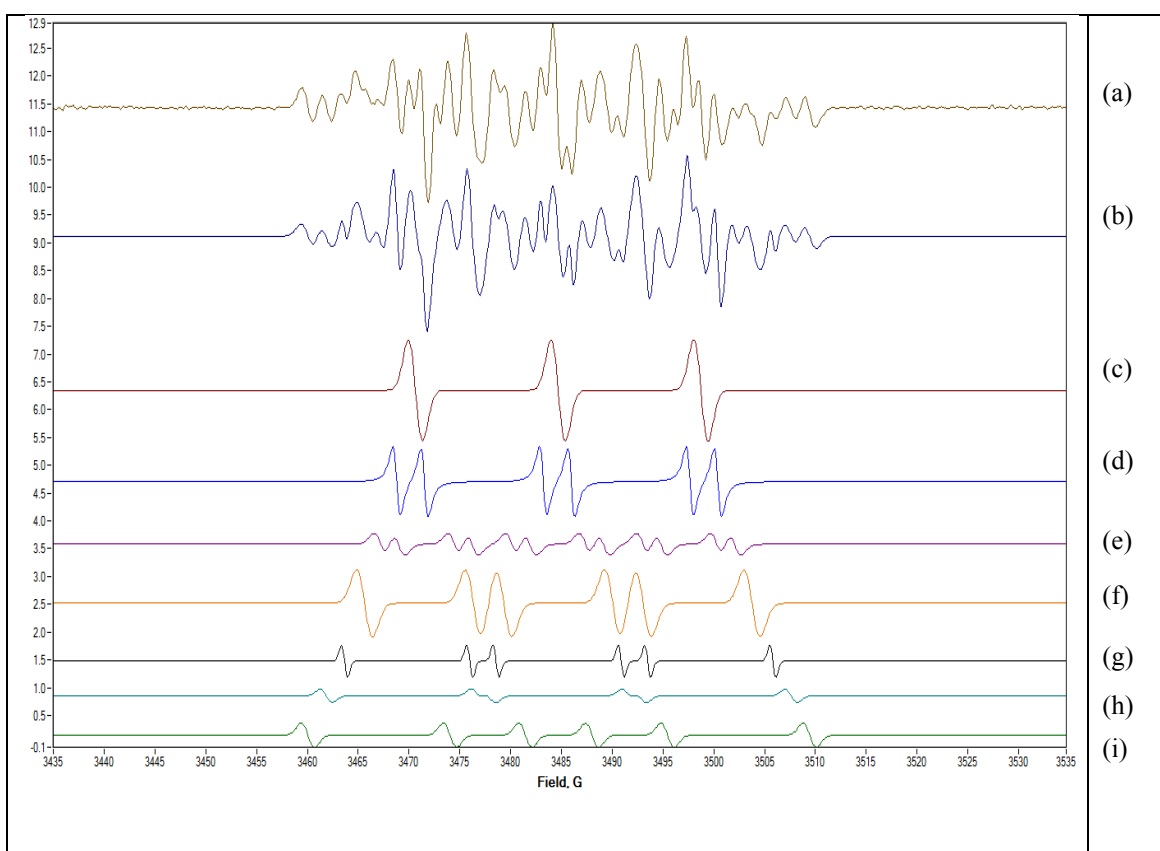


**Figure S2:** EPR spectrum deconvolution of the spin adducts obtained during cyclohexane oxidation over  $\text{MoO}_3$  at 180 °C in aerobic conditions. (a) experimental spectra and (b) simulated spectra. Several species can be identified:

(e) DMPO-O-C<sub>6</sub>H<sub>11</sub> spin adduct ( $a_N=12.85$ ,  $a_{H(\beta)}=7.24$ ,  $a_{H(\gamma)}=1.82$  G)<sup>2</sup>, (f) DMPO-OO-C<sub>6</sub>H<sub>11</sub> adduct ( $a_N=13.70$ ,  $a_H=10.70$  G)<sup>3</sup>, (g) DMPO-OH ( $a_N=14.90$ ,  $a_H=12.31$  G)<sup>4</sup>, (h) unidentified carbon centred radical adduct ( $a_N=14.82$ ,  $a_H=16.08$  G) and (i) DMPO-C<sub>6</sub>H<sub>11</sub> adduct ( $a_N=13.98$ ,  $a_H=21.39$  G)<sup>5</sup>.

Two further species were observed: (c) a species with  $a_N = 14.03$  G, which is a di-tert-butyl-nitroxide derivative, that can form by oxidation of DMPO<sup>6</sup> and a second species (d) with coupling constant  $a_N = 14.42$ ,  $a_H = 2.76$  G. Both of these could arise from the high amount of peroxy radicals present in solution.

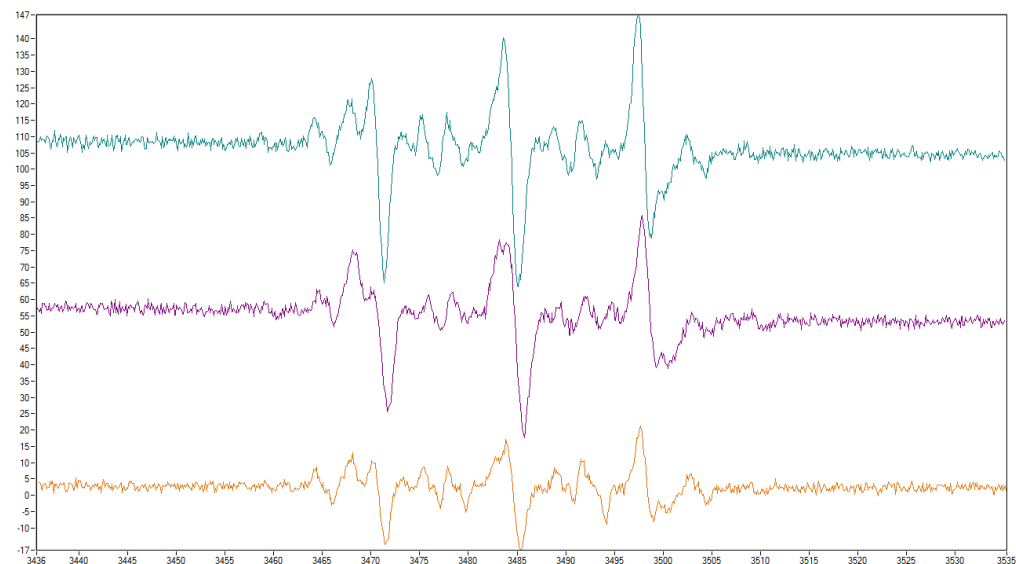


**Figure S3:** EPR spin trapping control experiments, using feeding the reactor with (—) cyclohexanol, (—) cyclohexanone and (—) reactor with no catalyst. In all cases a small amount of radicals is detected, containing mainly peroxy species.

### Lifetime of the radicals in gas phase

Evaluation of the lifetime of the trapped radicals is possible by evaluation of the spin adduct intensities measured under the same experimental conditions, but using reactor outlet of different length/diameter in order to increase the time of flight from the catalytic bed to the spin trapping solution. The following extension outlets were used: (a) 5 cm x 2.23 mm (ID), (b) 25 cm x 2.23 mm (ID) and (c) 10 cm x 10 mm (ID). This led to the increase of the time of flight from (a) 24.6 to (b) 61.5 and (c) 483.6 ms respectively. Evaluation of the intensities for  $C_6H_{11}-OO\cdot$ ,  $C_6H_{11}-O\cdot$  and  $C_6H_{11}\cdot$  spin adducts with DMPO, made it possible to obtain the following decays:

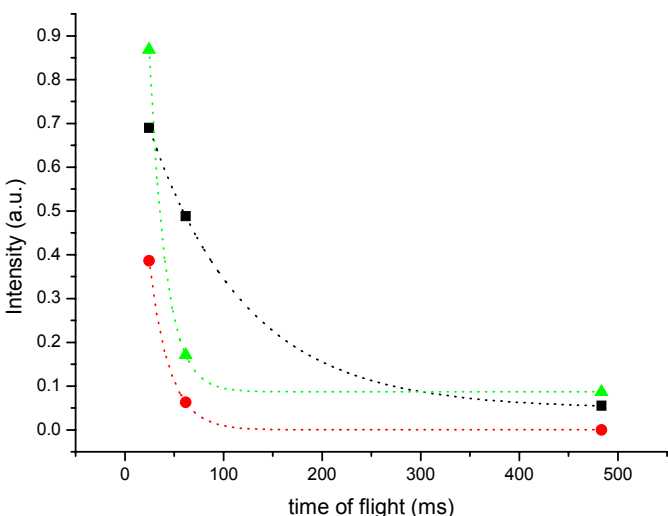


**Figure S4:** spin trapping intensity decay for (■)  $ROO\cdot$ , (●)  $RO\cdot$  and (▲)  $C_6H_{11}\cdot$  DMPO spin adduct moving from 24.6 to 483.6 ms of time of flight. The first order interpolation decay of the signal led to the following radical life time, expressed as  $t_{1/2}$ :  $ROO\cdot$  98 ms,  $RO\cdot$  17 ms and  $C_6H_{11}\cdot$  20ms.

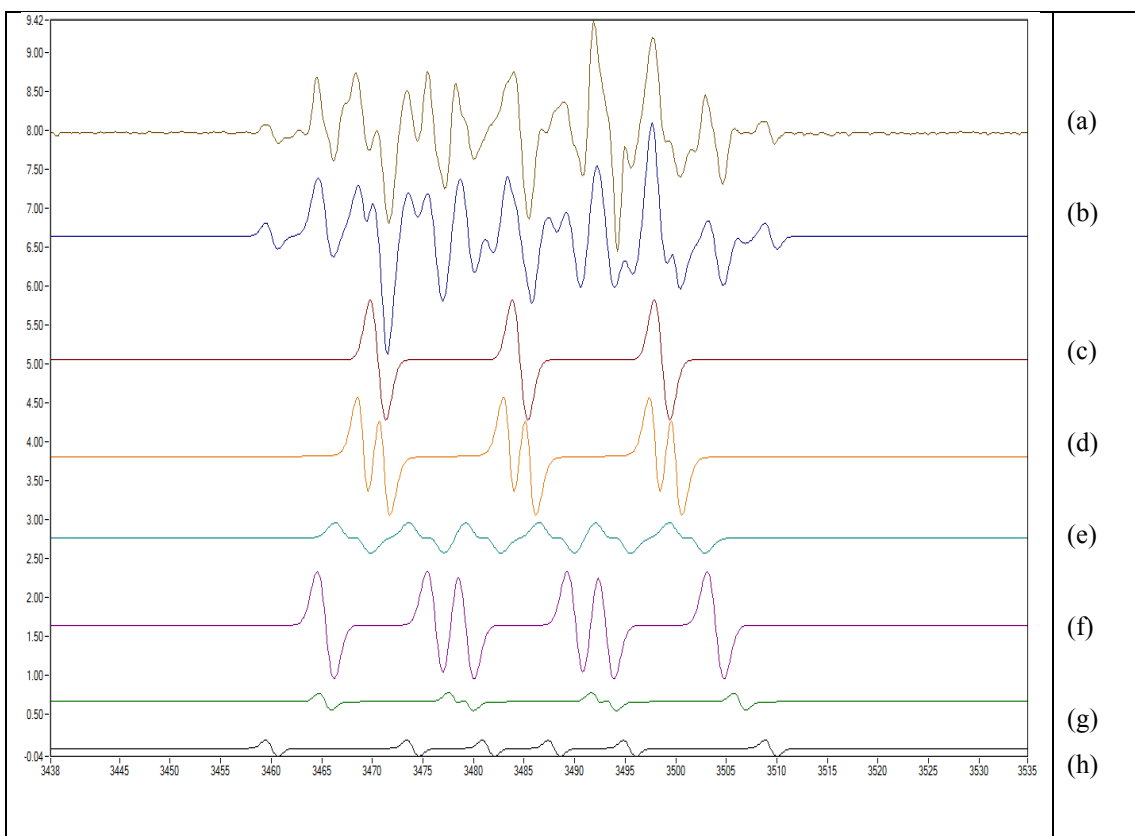


**Figure S5:** EPR spectrum deconvolution of the spin adducts obtained during cyclohexane oxidation over  $\text{MoO}_3$  at  $180\text{ }^\circ\text{C}$  in anaerobic conditions. (a) experimental spectrum and (b) simulated spectrum. (e) DMPO-O-C<sub>6</sub>H<sub>11</sub> adduct ( $a_N=12.85$ ,  $a_{H\beta}=7.30$ ,  $a_{Hy}=1.85\text{ G}$ ), (f) DMPO-OO-C<sub>6</sub>H<sub>11</sub> adduct ( $a_N=13.83$ ,  $a_H=10.87\text{ G}$ ), (g) DMPO-OH adduct ( $a_N=14.11$ ,  $a_H=12.74\text{ G}$ ) and (h) DMPO-C<sub>6</sub>H<sub>11</sub>( $a_N=13.95$ ,  $a_H=21.4\text{ G}$ ).

Also in this case DMPO derivative adducts are identified: (c) species  $a_N = 14.02\text{ G}$ <sup>6</sup> and (d)  $a_N = 14.42$ ,  $a_H = 2.02\text{ G}$ .

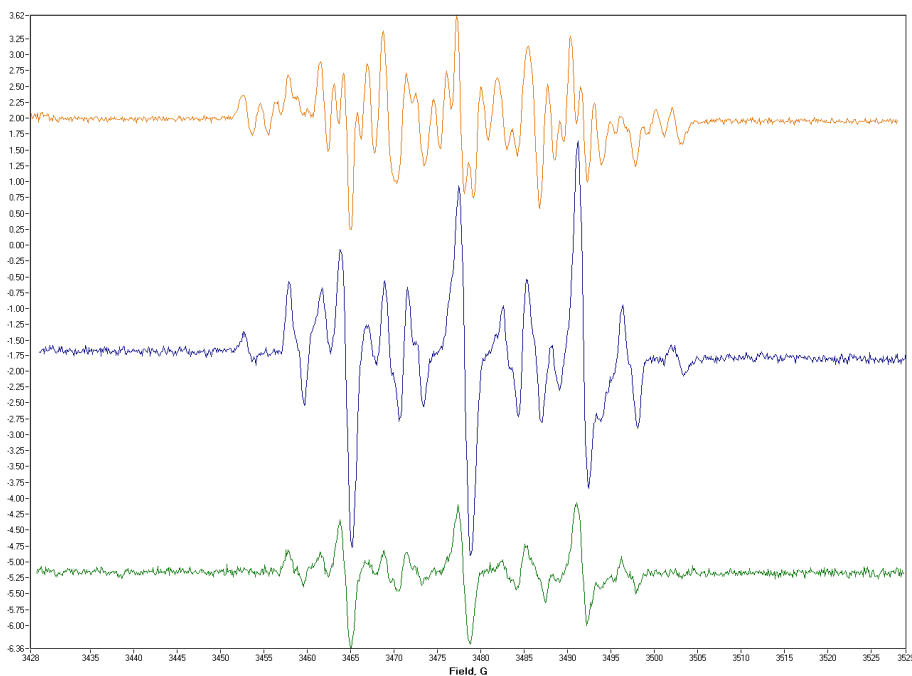


**Figure S6:** spin adducts spectra for the cyclohexane oxidation in air at 180 °C over: (—)  $\text{MoO}_3$ , (—)  $\text{Cr}_2\text{O}_3$  and (—)  $\text{WO}_3$ , using DMPO as spin trap. As long as the oxygen lattice mobility of the metal oxide decrease, a simplified spin adduct spectrum appears, up to disappearance of carbon and alkoxyl adduct and traces of peroxy adduct (the latter compatible with empty reactor)

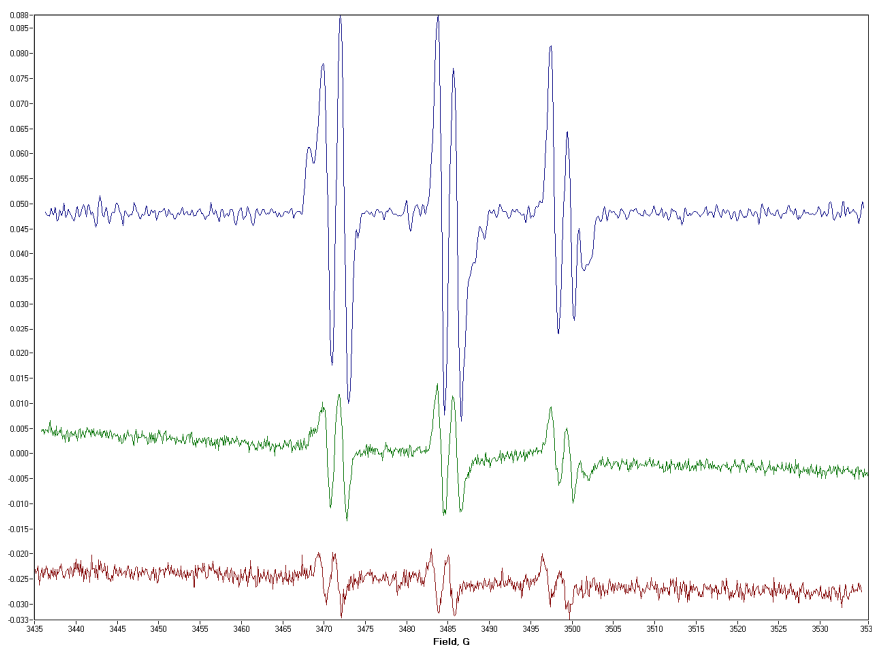


**Figure S7:** spin adducts spectra for the cyclohexane oxidation in air at 180 °C over: (—)  $\text{MoO}_3$ , (—)  $\text{Cr}_2\text{O}_3$  and (—)  $\text{WO}_3$ , using PBN as spin trap. Also in this case, as long as the oxygen lattice mobility of the metal oxide decrease, a lower spin adduct formation is detected. PBN allow to identify: peroxy species ( $a_N=13.69$   $a_H=1.83$  G)<sup>8</sup> and adducts of carbon-centred radicals ( $a_N=14.14$ ,  $a_H=3.60$  G)<sup>9</sup>

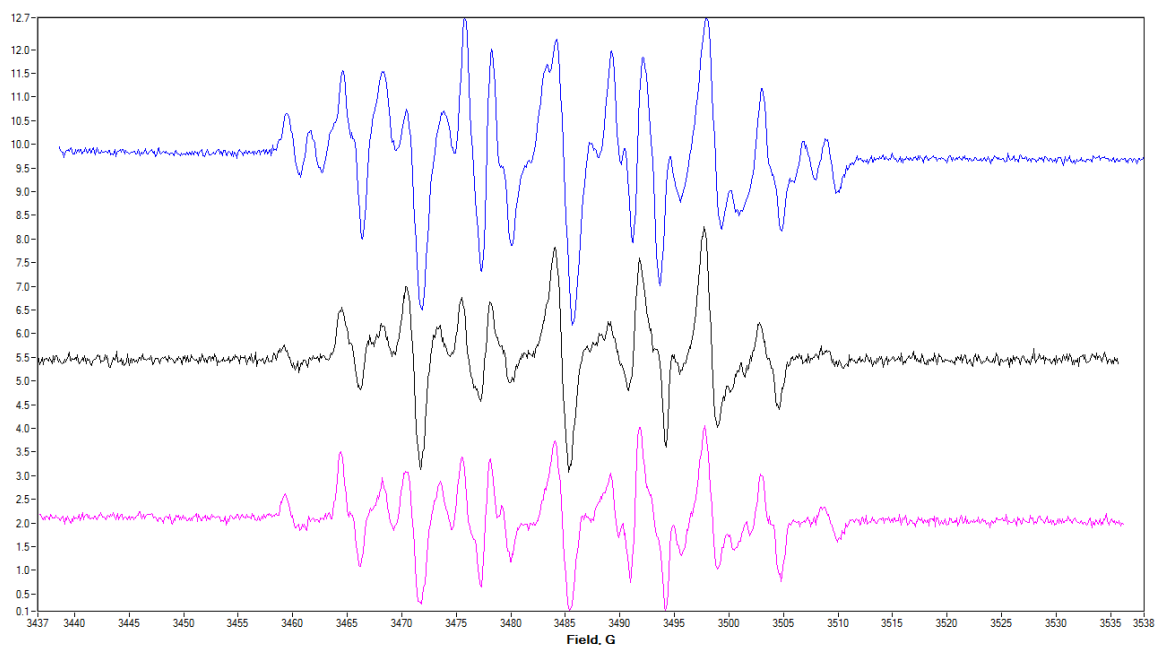


**Figure S8:** spin adducts spectra for the *n*-hexane oxidation in air at 180 °C over: (—) MoO<sub>3</sub>, (—) Cr<sub>2</sub>O<sub>3</sub> and (—) WO<sub>3</sub>, using DMPO as spin trap. Similarities with the species detected using cyclohexane as substrate are present: a ROO· adduct ( $a_N=13.67$ ,  $a_H=10.78$  G)<sup>2</sup>, a RO· adduct ( $a_N=13.11$ ,  $a_{H(\beta)}=8.24$ ,  $a_{H(\gamma)}=1.72$  G)<sup>3</sup>, ·OH ( $a_N=13.71$ ,  $a_H=12.33$  G)<sup>4</sup>, a carbon centred adduct characteristic of C<sub>6</sub>H<sub>11</sub>· ( $a_N=14.49$ ,  $a_H=20.30$  G)<sup>5</sup> and unidentified carbon centred radical adduct ( $a_N=14.19$ ,  $a_H=16.76$  G).

Also in this case DMPO derivative adducts are identified as in the case of cyclohexane: species  $a_N = 13.90$  G<sup>6</sup> and  $a_N = 14.22$ ,  $a_H = 2.34$  G.

However, it should be noted that investigation of the oxidation of *n*-alkyl species are much more challenging and beyond the current applicability of the spin traps used. In fact, in such case primary and secondary carbon centred radicals can easily be obtained with a wide series of products formation as well as decarboxylation of the substrate. Nevertheless, it is possible to observe a decrease in complexity of the spin adducts formation moving from MoO<sub>3</sub> to WO<sub>3</sub> thus supporting a general behaviour of these metal oxide versus alkanes oxidation with the common feature of incorporation of oxygen from the metal oxide lattice to the radicals involved in the oxidation reaction.

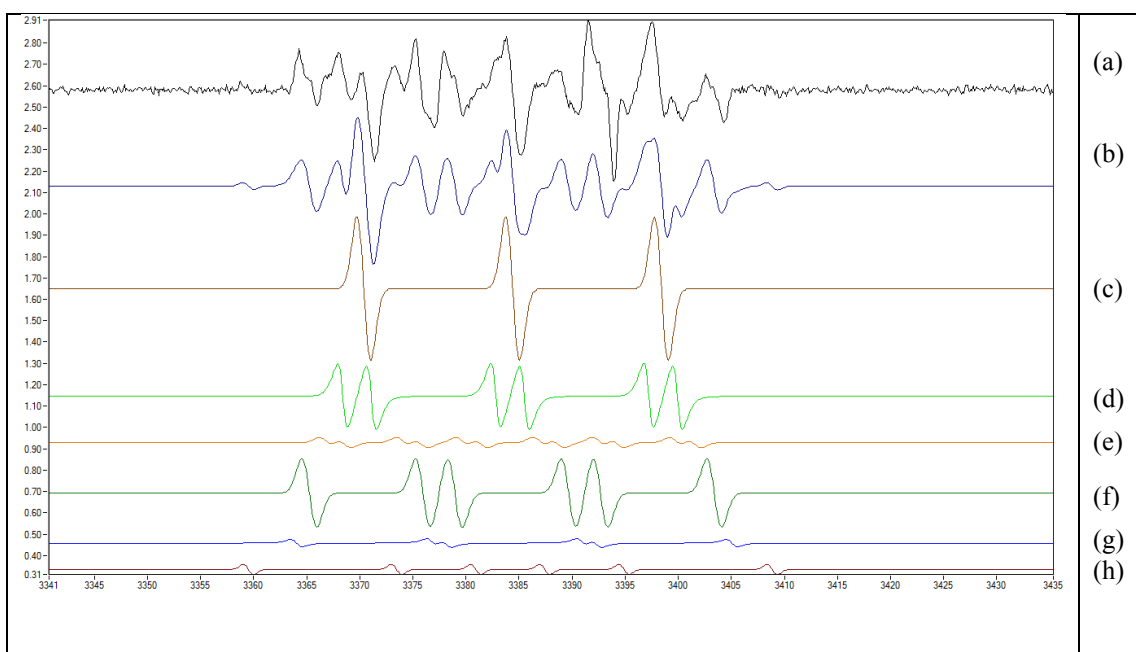


**Figure S9:** EPR spectrum deconvolution of the spin adducts obtained during cyclohexane oxidation over  $\text{MoO}_3$  at  $180\text{ }^\circ\text{C}$  for the spectra in **Figure 2a** of the manuscript main body. (a) experimental spectrum and (b) simulated spectrum. Several species can be identified:

(e) DMPO-O-C<sub>6</sub>H<sub>11</sub> spin adduct ( $a_N=12.85$ ,  $a_{H(\beta)}=7.24$ ,  $a_{H(\gamma)}=1.64\text{ G}$ ), (f) DMPO-OO-C<sub>6</sub>H<sub>11</sub> adduct ( $a_N=13.70$ ,  $a_H=10.70\text{ G}$ ), (g) DMPO-OH ( $a_N=14.90$ ,  $a_H=12.31\text{ G}$ ), and (h) DMPO-C<sub>6</sub>H<sub>11</sub> adduct ( $a_N=13.95$ ,  $a_H=21.40\text{ G}$ ).

Two further species are deconvoluted: (c) a species with  $a_N = 14.0\text{ G}$ , which is a di-tert-butyl-nitroxide derivative, that can occur by oxidation of DMPO<sup>6</sup> and a second species (d) with coupling constant  $a_N = 14.40$ ,  $a_H = 2.70\text{ G}$ .

## References

- 1) WinSim software is available through: <http://epr.niehs.nih.gov/pest.html>.
- 2) S. L. Baum, I. G.M. Anderson, R. R. Baker, D. M. Murphy and C. C. Rowlands, *Anal. Chim. Acta*, 2003, **481**, 1.
- 3) M. J. Davies and T. F. Slater, *Biochem. J.*, 1986, **240**, 789.
- 4) B. Kalyanaraman, C. Mottley and R. P. Mason, *J. Biochem. Biophys. Methods*, 1984, **9**, 27.
- 5) E. G. Janzen, C. A. Evans and J.-P. Liu, *J. Magn. Reson.*, 1973, **9**, 513.
- 6) A. G. Jantzen and B. J. Blackburn, *J. Am. Chem. Soc.*, 1969, **91**, 4481.
- 7) G. R. Buettner, *Free Rad. Biol. Med.*, 1987, **3**, 259.
- 8) N. Ohto, E. Niki, Y. Kamiya, *J. Chem. Soc., Perkin Trans. 2*, 1977, 1770.
- 9) W. A. Pryor, M. Tamura and D. F. Church, *J. Am. Chem. Soc.*, 1984, **106**, 5073.